# Deciphering the design of the tropomyosin molecule

**Jerry H. Brown*†, Kyoung-Hee Kim*†‡, Gyo Jun*§, Norma J. Greenfield¶, Roberto Dominguez‖, Niels Volkmann*,**, Sarah E. Hitchcock-DeGregori¶, and Carolyn Cohen*††**

*Rosenstiel Basic Medical Sciences Research Center, Brandeis University, Waltham, MA 02454-9110; ¶Department of Neuroscience and Cell Biology, University of Medicine and Dentistry of New Jersey–Robert Wood Johnson Medical School, 675 Hoes Lane, Piscataway, NJ 08854-5635; and ‖Boston Biomedical Research Institute, 64 Grove Street, Watertown, MA 02472

Contributed by Carolyn Cohen, May 3, 2001

**The crystal structure at 2.0-Å resolution of an 81-residue N-terminal fragment of muscle α-tropomyosin reveals a parallel two-stranded α-helical coiled-coil structure with a remarkable core. The high alanine content of the molecule is clustered into short regions where the local 2-fold symmetry is broken by a small (≈1.2-Å) axial staggering of the helices. The joining of these regions with neighboring segments, where the helices are in axial register, gives rise to specific bends in the molecular axis. We observe such bends to be widely distributed in two-stranded α-helical coiled-coil proteins. This asymmetric design in a dimer of identical (or highly similar) sequences allows the tropomyosin molecule to adopt multiple bent conformations. The seven alanine clusters in the core of the complete molecule (which spans seven monomers of the actin helix) promote the semiflexible winding of the tropomyosin filament necessary for its regulatory role in muscle contraction.**

Tropomyosin holds a special place in the history of protein structure. This two-stranded muscle protein has long been considered the archetype of α-helical coiled coils. These proteins have a sequence with a short-range seven-residue (so-called "heptad") repeat of the form (*a-b-c-d-e-f-g*), where *a* and *d* are generally apolar residues. The *a* and *d* residues form a left-handed apolar stripe along the surface of right-handed α-helices. The interlocking of these residues in a "knobs-into-holes" fashion by winding two (or three) helices around one another produces the coiled-coil molecule (1), which confers stability on highly charged polypeptide chains in an aqueous environment (for review, see ref. 2). Tropomyosin was the first α-helical coiled coil to be sequenced (3), and most isoforms (yeast excepted) have been shown to have an unbroken series of 40 continuous heptads, now known to be unusual in fibrous proteins. Analysis of this sequence also suggested that additional stabilization of the coiled coil was probably provided by salt links between residues *e* and *g* on neighboring chains, favoring a parallel in-register arrangement for two-chain molecules (4, 5). The core of the tropomyosin molecule (yeast excepted) is also unique among α-fibrous proteins in its unusually high content of alanine residues (≈35% in the *d* position in tropomyosin from vertebrate striated muscle) (6).

This basic design of a parallel dimeric α-helical coiled coil was confirmed by the crystal structure of the GCN4 "leucine zipper"—a relatively short α-helical coiled coil (7). This atomic resolution structure revealed that the two chains are in axial register, and that their side chains are arranged in alternating "layers" with distinctive orientations in the core *a* and *d* positions. The preferred rotamers adopted by the side chains permit their maximum close packing in the holes formed by four side chains of the neighboring helix. The simplicity of the linearly periodic coiled coil (in contrast to three-dimensional globular folds) has also permitted the visualization of conformational effects of different sequences or residues on most of the structural parameters of coiled coils, including pitch, parallel vs. antiparallel nature, and multimeric state (8–10).

Tropomyosin molecules bond head-to-tail with a short overlap (about nine residues) to form an essentially unbroken coiled-coil cable that winds around the actin helix: one tropomyosin molecule spans seven actin monomers in most muscles. In vertebrate striated muscle, myosin's contractile activity is controlled by a $Ca^{2+}$-sensitive complex of troponin and tropomyosin. The early two-state "steric blocking mechanism" (11, 12) has turned out to be the basic model for this regulation. Analysis of the tropomyosin sequence (4, 5) revealed a 14-fold repeat of surface acidic and apolar residues so phased that they may be pictured as corresponding to two alternate sets of seven quasiregular recognition sites for actin; these would be linked in the "off" or "on" states of contraction. Taking into account the flexibility of the molecule shown in crystallographic studies, Phillips *et al.* (13) then suggested a three-state model for regulation where tropomyosin's fluctuations influence thin filament cooperativity so that full activation requires a critical myosin occupancy. More recently, another three-state model has been advanced based on electron microscope studies of tropomyosin bound to actin where there is an additional small azimuthal movement of tropomyosin on the strong binding of myosin to actin [(14); see also ref. 15).

Native tropomyosin crystallizes in a number of forms that have yielded relatively low-resolution structures at, successively, 15 Å in one form (13, 16) and 9 Å (17) and 7 Å (18) in another. To achieve high resolution, we have attempted to crystallize shorter fragments of the molecule. Here we describe the crystal structure to 2.0-Å resolution of a recombinant (unacetylated) modified 81-residue N-terminal peptide of chicken striated α-tropomyosin (subsequently referred to as "Tm81"). The results reveal the effects of clusters of core alanines on the axial register, symmetry, and conformational variability of two-stranded coiled coils that appear to be important for tropomyosin's role in the regulation of muscle contraction.

## Methods

**Protein Expression and Purification.** A plasmid encoding Tm81 was prepared by altering the tropomyosin cDNA to introduce a stop codon (UAG) at residue 82, and changing Ala-81 to Cys. Site-specific mutagenesis was carried out as described elsewhere (19–21), by using the oligonucleotide:

5′-GGCCACAGAT**TG**T**T**AGAGTGAAGTAGCT-3′.

The protein was expressed in *Escherichia coli* and purified as described (20, 22), with modifications.

**Crystal Structure Determination.** The Tm81 peptide was crystallized in space group P1 (a = 41.4 Å, b = 45.5 Å, c = 56.3 Å, $\alpha$ = 93.7°, $\beta$ = 98.1°, $\gamma$ =104.4°) with two dimeric molecules per unit cell

Data deposition: The atomic coordinates have been deposited in the Protein Data Bank, www.rcsb.org (PDB ID code 1IC2).

See commentary on page 8165.

†J.H.B. and K.-H.K. contributed equally to this work.

‡Present address: Life Science R&D, LG Chemical Ltd./Research Park 104-1, Moonji-dong, Yusong-gu, Taejon 305-380, South Korea.

§Present address: Gachon Medical School, Kang Hwa, Inchon 417-840, Korea.

**Present address: The Burnham Institute, 10901 North Torrey Pines Road, La Jolla, CA 92037.

††To whom reprint requests should be addressed. E-mail: ccohen@brandeis.edu.

The publication costs of this article were defrayed in part by page charge payment. This article must therefore be hereby marked "*advertisement*" in accordance with 18 U.S.C. §1734 solely to indicate this fact.

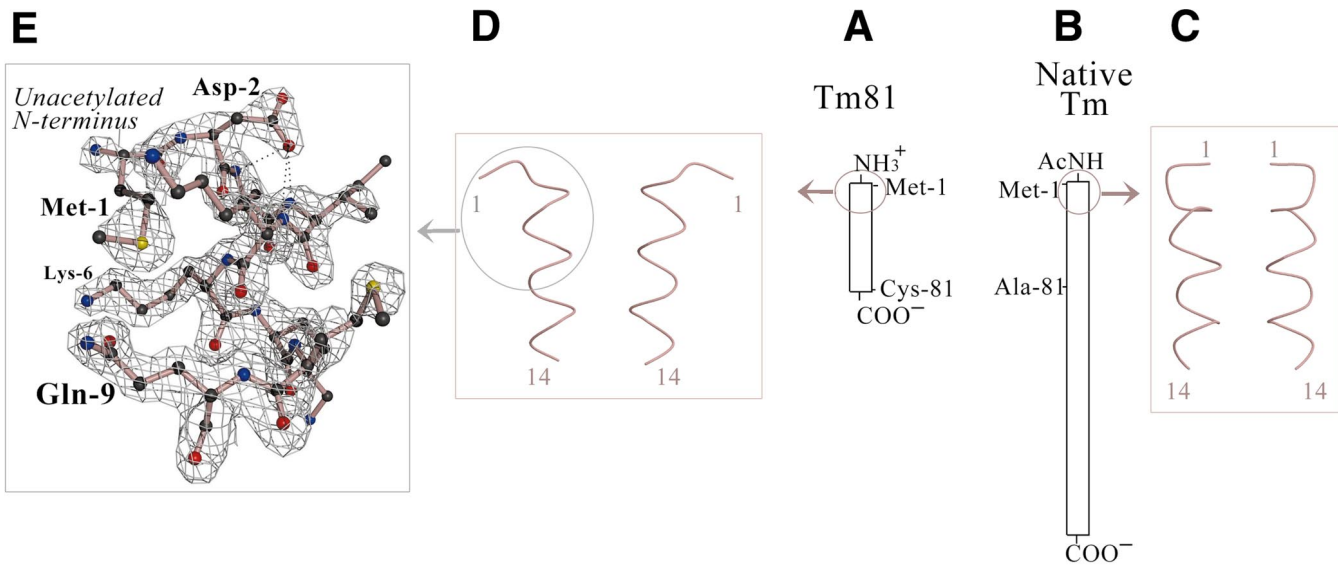


**Fig. 1.** Differences between native tropomyosin (*B*, *C*) and the Tm81 construct (*E*, *D*, *A*). (*A*, *B*) Sketches showing how the first 81 residues of native $\alpha$-tropomyosin differ from the Tm81 fragment at their N and C termini (also see *Methods*). (*C*, *D*) $\alpha$-Carbon drawing of the N-terminal 14 residues of the fully helical N-acetylated TmZip NMR structure (23) and of the unacetylated Tm81 crystal structure, in which residues 1 and 2 are nonhelical. (*E*) The nine N-terminal residues of Tm81. The coordinates are those of the final refined model. Residues C1–C9 are shown. The electron density map is shown within 2.0 Å of each atom at a contour level 1.75 $\sigma$. It was produced by using $2F_o - F_c$ coefficients and phases calculated from a preliminary (and fully helical) model (similar to *C*) early on in the refinement procedure. This ''omit''-style map for residues 1 and 2 reveals their nonhelical path, which is the same for all four chains of the asymmetric unit. At the unacetylated terminus of each Tm81 chain, the Met-1 side chain contacts surface residues 5, 6, and 9, and Asp-2 stabilizes the three exposed main-chain amino groups of residues 3, 4, and 5 at the N terminus of the $\alpha$-helix. Drawings are made by using POVRAY (www.povray.org) and a version of MOLSCRIPT (46) modified to read maps by E. Peisach.



(referred to as "AB" and "CD"). The structure was solved by a combination of molecular replacement [using coiled-coil search models (7, 13)] and single isomorphous replacement (using a trimethyllead-acetate derivative). This solution (and register) for all four chains in the unit cell were also confirmed by high-quality omit electron density maps (see, for example, Fig. 1). Data statistics are found in Table 1. Additional protein expression, purification and crystallographic methods are published as supplemental data on the PNAS web site, www.pnas.org.

## Results

**Overall Structure.** The fragment is almost completely $\alpha$-helical, except for a few residues at the ends, both of which have non-native modifications. To crystallize this peptide, the C termini were crosslinked by a disulfide bond. As a likely consequence, residues 76 to 81 are relatively disordered and appear to form a hairpin loop in one molecule of the asymmetric unit and a coiled coil in the other. More significantly, because bacterial expression was used, the N termini of this expressed peptide are not acetylated, in contrast to native tropomyosin. In the crystal structure, residues 1 and 2 are in extended conformations (Fig. 1), whereas an NMR study of a chimeric peptide including the acetylated N-terminal 14 residues of tropomyosin peptide indicates a fully helical structure (23). This change in structure because of *N*-acetylation confirms previous predictions (24) and circular dichroism studies (25) and is consistent with the critical role of *N*-acetylation (26, 27) [or other extensions of the peptide at the N terminus (24)] for tropomyosin filament formation and actin affinity. The remainder of the Tm81 peptide forms an $\alpha$-helical coiled coil that in many respects has a canonical structure. The two chains wind halfway around each other in ≈52–54 residues (or ≈78–81 Å), which is slightly longer than the average half-pitch length (70 Å) reported for the native filament at 9-Å resolution (17). The distance between the helical axes in the coiled coil varies from ≈8 Å in the region between residues 15 and 36, which is rich in small and unbranched core side chains (see below), to ≈9.5–10 Å in most of the remainder of the peptide. The few residues near the unacetylated N terminus are slightly splayed. In addition to apolar core interactions described

**Table 1. Statistics for x-ray structure determination**

| | Native | $(CH_3)_3PbOAc$ |
|---|---|---|
| Data collection | | |
| Resolution | ∞ − 2.0 | 50–2.8 |
| Redundancy | 10.0 | 2.8 |
| No. of unique reflections | 26,797 | 9,234 |
| Completeness, % | 99.9 | 95.5 |
| $R_{sym}$* | 8.7 | 6.6 |
| Heavy atom phasing | | |
| $R_{iso}$ | | 10.8 |
| No. of binding sites | | 4 |
| Phasing power | | 0.83 |
| Mean figure of merit | | 0.23 |
| Refinement (∞ → 2.0-Å resolution) | | |
| $\sigma$ cutoff | None | |
| Number of protein/water atoms | 2,489, 178 | |
| *R* factor† %, *R* free‡ % | 24.8, 28.3 | |
| rms bond length, Å, angles, ° | 0.0066, 0.88 | |
| rms dihedrals, °, improper, ° | 13.17, 0.62 | |
| Coordinate errors, Å | | |
| Luzatti, crossvalidated Luzatti | 0.28, 0.35 | |
| Average *B* factor | | |
| All atoms | 44.8 | |
| Molecule AB (main, side) | 39.6 (34.0, 45.3) | |
| Molecule CD (main, side) | 50.8 (45.2, 56.5) | |

*$R_{sym} = \Sigma_{hkl}\Sigma_i|I_i - \langle I\rangle|/\Sigma_{hkl}\Sigma_i I$; where $\langle I\rangle$ is the mean intensity of reflection hkl.
†*R* factor $= \Sigma_{hkl}||F_{obs}| - |F_{calc}||/\Sigma_{hkl}|F_{obs}|$; where $F_{calc}$ and $F_{obs}$ are, respectively, the calculated and observed structure factor amplitudes for reflection hkl.
‡*R* free is the same as *R* factor but calculated over the 5% randomly selected fraction of the reflection data not included in the refinement.

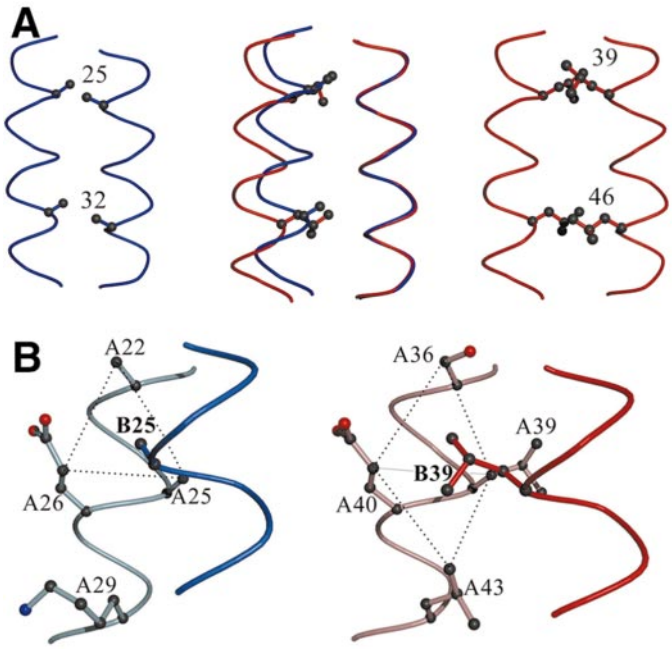


**Fig. 2.** The ''alanine stagger.'' (*A*) A parallel two-stranded coiled-coil segment rich in core alanines, such as Tm81 (fragment ''AB'') residues 22–36 (*Left*) is axially out-of-register by ≈1.2 Å and narrower by ≈2 Å compared with a canonical 2-fold symmetric segment dominated by core leucines, such as Tm81 residues 36–50 (*Right*). The superposition (*Middle*) shows that this difference in the axial and radial dispositions of the α-helical backbones in the two segments causes the relative locations of their core side chains' terminal methyl groups (i.e., the Cβ atoms of alanine residues 25 and 32 and the Cδ1 atoms of leucine residues 39 and 46) to be nearly the same (within 0.59 and 1.09 Å, respectively). (*B*) The terminal methyl groups in both types of core, such as Tm81 alanine 25 (*Left*) and leucine 39 (*Right*), make contacts with at most three residues in a triangular ''hole'' of the neighboring helix. [As published as supplemental data on the PNAS web site, www.pnas.org, a similar axial staggering of the helices occurs in this region and in the (modified) second alanine cluster of the other (''CD'') fragment of the asymmetric unit; here differences are also described in the extent of axial staggering near the modified N and C termini between the two fragments located in different crystal environments.]

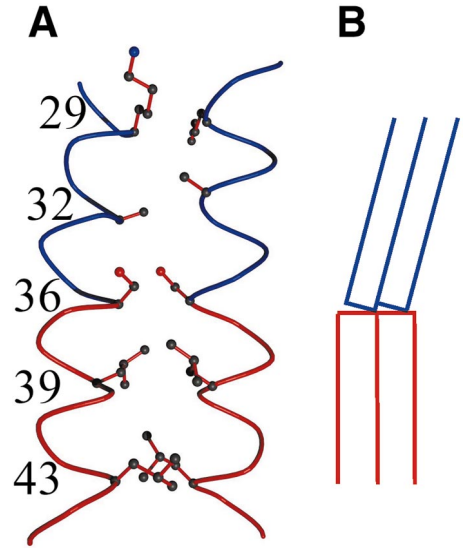


**Fig. 3.** The ''alanine bend.'' (*A*) The joining of an axially staggered coiled-coil segment, such as Tm81 (fragment ''AB'') residues 28–36 (blue), and an unstaggered segment, such as residues 36–45 (red) produces a bend of the coiled-coil axis (here at ≈ residue 36) away from the locally longer α-helix (*Left*). The structure of this region is nearly identical in the two crystallographically independent fragments. (Similar bends also occur at ≈ residues 22 and 68 in the ''CD'' fragment, as shown in the supplemental data, which also describes how supercoiling results in the coiled-coil axis at the two boundaries of a staggered segment to bend in different planes.). (*B*) Simplified schematic of the joint.

below, two types of ionic interactions between the neighboring helices stabilize this coiled coil: canonical salt linkages between side chains in the *e* and *g* positions (4, 28) (residues R21-E26, K35-E40, and K49-E54 in both the 8- and 10-Å-wide portions) and rarer ones between the *g* and *a* positions (28, 29) (residues D14-K15 and D28-K29, found only in the 8-Å-wide region of the coiled coil).

**The Alanine Stagger and Bending of the Coiled Coil.** An unusual feature of the tropomyosin peptide, which we now recognize because of the high resolution of this structure, is that the two chains of the coiled coil are axially out of register by ≈1 Å in certain regions along its length (Fig. 2 and supplementary data, www.pnas.org). The cores of these segments are distinctive and predominantly composed of alanines and other unbranched residues, and each side chain contacts three residues at most from the neighboring helix (Fig. 2). The axial shift breaks the local 2-fold symmetry of the structure, so that the two neighboring α-helices, despite their identical sequences, are in different chemical environments. In this way, each core side chain ("i") from the C-terminally shifted α-helix contacts a C-terminally displaced set of residues (i′, i′ + 1, and i′ + 4), whereas the reciprocal contact of i′ is made with a different relatively N-terminally displaced set of residues (i − 3, i, and i + 1). These ''alanine-staggered'' regions contrast with the remaining more canonical segments of the Tm81 coiled coil that are dominated by core leucines, which contact four residues of the opposing chain. Here, the two α-helices are in-register and are related by a parallel diad.

The places where the axially shifted and in-register regions join one another are also the locations of relatively sharp bends (on average ≈6°) in the axis of the coiled coil (see Fig. 3 and legend). Each junction may be pictured as being similar to that which would occur if there were a local insertion of almost one residue in one helix relative to the other helix. In this way, the joining of two such segments specifies the bending of the coiled-coil axis away from the effectively longer helix, much as a bend in a multilane track consists of longer outer lanes. Bending a coiled coil by alternating clusters of core alanine and leucine residues appears to be a general design in α-helical bundles and coiled coils: we have also identified this type of junction and bend in the antiparallel α-helical bundle of the ColE1 rop protein (30) at residues 20 and 40, and in the parallel two-stranded coiled coil of cortexillin (31) at residue 332. The bends in these coiled coils are primarily confined to ≈1–1/2 helical turns and affect the lengths of only two to three pairs of consecutive main-chain hydrogen bonds; this result is consistent with the observation in cortexillin that even a very short "cluster" of one core alanine can produce a similar effect.

## Discussion

**Knobs-into-Holes Redefined on an Atomic Level.** Surveys of α-helical interactions in globular proteins (32) and antiparallel coiled coils (33) have revealed distinct sites or "holes" where leucine and alanine residues prefer to bind. The centers of these two (overlapping) cavities are axially separated by ≈1.5 Å, and the two interacting helices are consequently in somewhat different relative axial relationships, depending on the predominant residue in the core (33). Superpositions of interacting helices with different relative axial shifts, by using both parallel (Fig. 2*A*) and antiparallel coiled coils as examples, reveal, however, that both the alanine- and

leucine-dominated cores, which appear to be dissimilar, are in fact close packed in a similar way at the atomic level.

In the conventional description (1), a side chain from one helix fits into a "hole" formed by four residues of the neighboring helix; any particular atom, however, generally contacts three residues at most. This interaction occurs because the four-residue "hole" actually takes on an acute diamond-shaped form (Fig. 2*B*), in which residues i′ − 3 and i′ + 4 are generally too far apart to be spanned by a single atom or a single methyl group. This hole can then be alternatively visualized as consisting of two adjoining nearly equilateral triangle-shaped halves, one (i′ − 3, i′, i′ + 1) axially staggered "up" and the other (i′, i′ + 1, i′ + 4) staggered "down" (33). Close inspection of the core leucine residues 39, 43, 50, 57, and 64 of Tm81 as well as 5, 12, and 19 of GCN4 reveals that their side-chain conformations displace the two terminal methyl groups axially relative to one another (Fig. 2*B*). These two methyl groups from one helix are in a correct axial position to fit into the two adjoined triangular halves of the four-residue hole when the two (parallel) chains are "unstaggered" and in-register. The branched nature and length of the leucine side chains thus appear to be partly responsible for the proper 2-fold relationship observed between these parallel α-helices. In the segment of Tm81 that lacks branched aliphatic residues in the core, the helices are shifted relative to one another so that they are slightly out of register, to place the lone terminal methyl group into a triangular hole. This pattern is in fact a general description of the knobs-into-holes interaction at the atomic level.[‡‡]

**Structure of Native Molecule: Periodic Repeats and Localized Features in the Core.** The role of *d*-position alanines in the structure of Tm81 has important implications for the native molecule. It had previously been noted that, in contrast to other α-fibrous proteins, alanine is the most common residue in the core *d* position of vertebrate tropomyosins (≈35% in the rabbit α and β chains, equine platelet and chicken gizzard α and β chains) (6). Inspection of the sequence of vertebrate striated α-tropomyosin (Fig. 4) shows that these residues are clustered into seven groups (of one to three *d*-position alanines each), which are separated from one another by segments of slightly varying lengths rich in *d*-position leucines. (Similar clusters are observed in tropomyosin isoforms encoded by different genes and expressed in different tissues.) The compositions of the *a* positions of these "alanine clusters" are also distinctive in sharing a low occurrence of valine and isoleucine residues (Fig. 4). These aliphatic β-branched side chains [which are relatively common in the *a* positions of canonical ≈10 Å-diameter two-stranded coiled coils (6, 8)] appear by model building to be too bulky for an ≈8-Å diameter coiled coil. These results suggest a model for the native molecule that consists of seven pairs of alternating canonical and narrow/staggered segments of coiled coil that relate to the winding of the tropomyosin filament around the actin helix (see below). Although the alanine clusters are not evenly spaced along the tropomyosin molecule, as are the seven (so-called "α") recognition sites for actin on the surface of the molecule (4, 5, 13), they are distributed throughout the length of the molecule. The quasiregular binding of one tropomyosin molecule to seven actin monomers is thus expressed in the core of this coiled coil as well as in the sequence on its surface.

Certain features of the core sequence, however, differentiate the alanine clusters from one another, both within a tropomyosin molecule and between different isoforms, and may also play a role in enhancing the aperiodic localized properties of tropomyosin. Near the N terminus, for example, the first cluster, which is intact in Tm81, is unique in being stabilized by interhelical salt linkages between the core *a* and flanking *g* positions, and in lacking *a* position leucines. The N-terminal three clusters are also longer (three *d* alanines in a row) and spaced a bit more regularly than are the C-terminal four alanine clusters (one or two *d*-position alanines each). Near the C terminus, the seventh "cluster," which consists simply of one *d*-position alanine at residue 277, is unique in having no accompanying *a*-position alanine. On the surface, small differences in the amino acid composition also occur among the seven α-zones and to a greater degree among the less regular seven β-zones (5). The core and the surface of tropomyosin probably function together in defining specialized roles of different regions of the molecule. These include the specialized sites in the C and N termini of the molecule that produce the critical head-to-tail overlap in the filament and the specific binding site for troponin T within residues 258 to 275 near the C terminus of striated-muscle tropomyosin (34). Moreover, the specificity of troponin T for binding only striated-muscle tropomyosin (35) is consistent with these residues being markedly different (both in the core and on the surface) in the different isoforms (Fig. 4). Additional structural consequences of these C-terminal sequence differences will be described elsewhere (Y. Li, S. Mui, L. Tobacman, L. Reshetnikova, J.H.B. & C.C., unpublished data). In contrast to these vertebrate isoforms, tropomyosin from yeast [e.g., TPM1 (36)] does not have clusters of *d*-position alanines; moreover, yeast tropomyosin is distinctive in having breaks in its heptad repeat (L. Tobacman, personal communication). These interruptions probably provide the flexibility that, in the absence of core alanines, may be necessary for the molecule's binding to actin.

**Multiple Conformational States and the Regulatory Mechanism.** The distinctive structure of tropomyosin reveals unusual dynamic properties that we believe are important in the regulatory mechanism of muscle contraction. In attempts to account for the flexibility of coiled coils, one of the simplest pictures had been based on a model of a uniform, symmetric, and straight molecule with one lowest energy conformation (37). In this case, thermal energy alone (or binding of another molecule) would allow deformations such that the rod could be gradually bent (38). We now recognize, however, that in the case of (vertebrate) tropomyosin, the core alanines stabilize specific and sharp asymmetric bends in the axis of the coiled coil. (In the Tm81 crystal structure, the temperature factors of the intact alanine cluster and associated bends are not higher than those in the adjoining canonical segments.) Moreover, the strictly homodimeric nature of α-tropomyosin means that in this case the coiled coil will have an equal tendency (assuming no external constraints) to bend in either of two opposite directions at the junctions of each alanine cluster, depending on which of the two helices is shifted toward the N terminus. (Compare, for example, the first and second alanine staggers in Fig. 4*B*.) The highly elongated nature of the molecule and the unstaggered 2-fold symmetric nature of the intervening canonical segments observed in the Tm81 structure also make it unlikely that the sense of bending around one alanine cluster should affect the bend at the next one, so that isolated α-tropomyosin would be able to adopt and be stabilized in multiple (up to $2^7$ or 128) bent conformations of roughly equal energy.[§§]

[‡‡]This concept may be tested, for example, by extending the structural surveys of interhelical interactions (32, 33), to include the precise positions of side-chain functional groups.

[§§]In the striated-muscle αβ-tropomyosin heterodimer, the sequence identity is 86%, and most of the differences involve chemically similar amino acid residues (39), so that a similar situation will probably obtain. Note, however, that the remaining amino acid differences, some of which occur in a number of the joints, may bias the bending in certain cases, possibly diminishing to some extent this type of alanine-induced conformational variability relative to the homodimer. In vertebrate skeletal muscle, both αα and αβ dimers are present, whereas in vertebrate smooth muscle, the αβ heterodimer is the predominant species (35). The important point is that the joints provide the basis for striking conformational variability whether the tropomyosin dimer consists of identical or highly similar chains.

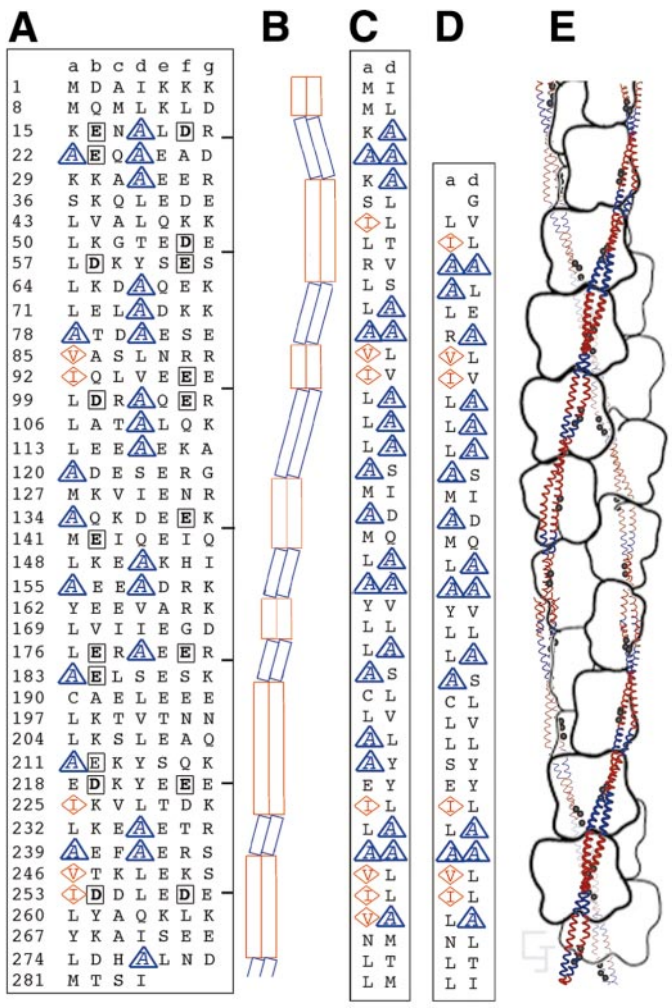


**Fig. 4.** Similarities and differences in the core amino acid sequences of both muscle and nonmuscle isoforms. (*A*) The 284-residue long sequence of chicken striated $\alpha$-tropomyosin (SWISS-PROT P02559) shows that there are seven clusters of *d*-position alanines (highlighted by blue triangles) in addition to the relatively regular negatively charged surface residues in the $\alpha$-zones (4, 5) (bold in black square, and dashes to the side). These $\alpha$-zones are implicated in the binding of tropomyosin to seven actin subunits. Note that *a*-position $\beta$-branched residues (highlighted in red diamonds) are common in canonical coiled-coil segments (see *Discussion*) but rare in the alanine clusters of this and other tropomyosin isoforms. (*B*) Simplified schematic diagram (supercoiling not depicted) of one of many (up to $2^7 = 128$) possible discrete conformations for tropomyosin that can be produced by the alternating seven alanine (blue staggered rectangles) and canonical (red in-register rectangles) *d*-position clusters. The fourth and fifth ''canonical'' segments are unusual in not having any *d*-position leucines. (*C*) As *A*, but only the core sequence of native $\alpha$-tropomyosin from smooth muscle of chicken gizzard (SWISS-PROT P04268) is shown. These two alternatively spliced tropomyosin isoforms are encoded by the same gene and are identical except for exon 2 (residues 39-80) and exon 9 (residues 258-284). Similar alanine clusters are encoded by exon 2 of these two tropomyosin isoforms; in contrast, the last *d* position alanine in exon 9 is not conserved between these isoforms, corresponding to the general divergence of the sequences in the C-terminal region (47), which is the apparent binding site (only in skeletal muscle tropomyosin) for troponin T. In general, the alanine clusters are conserved in tropomyosin isoforms encoded by different genes. (*D*) Many of the alanine clusters are also present in the core sequence of the shorter 248-aa residue nonmuscle human fibroblast tropomyosin (SWISS-PROT P07226), which binds only six actin subunits and is a $\delta$ tropomyosin encoded by the TPM4 gene. Note that in this figure we have not attempted to align the first six heptads of this sequence with the other sequences shown. (*E*) A model of the native tropomyosin molecule and filament generated from the Tm81 coordinates (see supplemental data, www.pnas.org) and a simplified model of the actin helix [drawn by Graham Johnson (fivth.com)]. The black spheres correspond to the periodic surface acidic residues of the $\alpha$-zones. [The scale of a tropomyosin molecule is different from those in *A–D*. Note that the precise structure is unknown for the head-to-tail overlap between two consecutive tropomyosin molecules in a filament (located about two-thirds down the figure)].

This general design clarifies the physical basis for various models of regulation that envisage both conformational variability and flexibility (or ''semiflexibility'') of this molecule. There is now good evidence that $Ca^{2+}$-dependent regulation of muscle contraction by tropomyosin and troponin consists of three average functional states for the thin filament: an ''off'' (or ''blocked'') state, which does not bind myosin and therefore does not activate the myosin-ATPase activity, a $Ca^{2+}$-induced ''on'' (or ''closed'') state, which allows weak binding of myosin heads and a low ATPase activity, and a ''fully active'' (or ''open'') state that leads to strong myosin binding and maximum ATPase activity (15, 40). Correspondingly, tropomyosin has been observed by electron microscopy to take up, on average, three different azimuthal positions (separated by $\approx$5–10 Å) on the actin helix, depending on the presence of $Ca^{2+}$ and the concentration of myosin heads (14, 41). These positions involve contacts with different regions of the actin surface and therefore require at least three different accessible conformations for the tropomyosin coiled coil. Our results indicate that bending and conformational variability should be specifically promoted and stabilized by the unique design of this molecule.

Additional conformational variability of the tropomyosin filament arises from the cooperative nature of myosin binding to the thin filament. A key factor is that the strength of the head-to-tail overlap of two successive tropomyosin molecules determines the cooperative length of the filament (42). Electron microscopic studies of S1-decorated thin filaments (14) have shown that on average the binding of about two myosin heads per seven actin monomers affects the position of the tropomyosin filament on actin up to $\approx$1,200 Å from the limited region of decoration (see also refs. 38 and 42). The limited cooperative length requires distinctive connecting paths along the filament between regions of tropomyosin that are in different functional states. The length of such paths appears long in the electron microscope images (14); in contrast, however, the sharpness of the bends observed in the Tm81 crystals is consistent with a tropomyosin filament that can bind, say, the off site of one actin monomer and the activated site of the next monomer of the actin helix. This ability of tropomyosin to change its position locally on the thin filament agrees with recent myosin-thin filament binding studies that used tropomyosin internal deletion mutations (43).

The physiological importance of the sequence in the core has in fact recently been demonstrated. A form of hypertrophic cardiomyopathy is caused by a valine-to-alanine mutation at the *d*-position 95 of $\alpha$-tropomyosin (44), which extends the length of the molecule's third alanine cluster. The abnormal myosin cycling and calcium binding to troponin associated with this disease are thus consistent with the importance of this region in thin filament activation. These results suggest that the specific locations of the bends promoted by core alanines are also important for tropomyosin's normal function.

**Perspective.** Our results provide information on both the general features of $\alpha$-helical coiled-coil structures and the specialized design of the tropomyosin molecule related to the regulation of muscle contraction. Just as crystallographic studies of GCN4 mutants have shown how the special shapes of certain apolar residues, such as leucines and isoleucines, can determine the stability and multimeric state of the structure (8), we describe here how the packing of alanine clusters in the core of tropo-

myosin affects the local symmetry and bending of the molecule. The small axial shift of $\alpha$-helices caused by core alanines has the effect of breaking the chemical equivalence of the two chains without requiring two different amino acid sequences. A similar axial shift and bending because of alanine residues also occur in a variety of antiparallel coiled coils such as those in the ColE1 rop protein. Note, however, that in contrast to such asymmetric structures composed of two different sequences, asymmetry in a homodimer, whether caused by core alanines or some other motif, can generate and stabilize a number of different (albeit related) conformations under the same conditions.

The tropomyosin molecule—often considered to be the paradigm for $\alpha$-helical coiled coils—has, in fact, now been shown not only to have a specialized design on the surface but also in the core for its functional role in muscle. In the early two-state versions of the steric blocking mechanism, a simple quarter-turn rolling of a regular, symmetrical, rigid tropomyosin molecule on the actin helix (promoted by the binding of $Ca^{2+}$ to troponin) was pictured as sufficient to account for the switch from the "off" to the "on" state of contraction (5, 45). In a later three-state model (13), the weak binding of the more regular surface sites on tropomyosin to actin and the decreased flexibility of the molecule on the strong binding of myosin to actin were recognized as key features of the regulation. Our present results clarify the physical basis for this flexibility. They also indicate that the tropomyosin filament moves in a jointed or "segmented" manner on the actin helix rather than by a rigid rolling motion, and that it has the potential for many conformational states. But many aspects of this mechanism have yet to be established. One puzzle is the presence of three azimuthal positions on actin for a tropomyosin molecule, which appears to have but two sets of surface binding sites (5, 14, 41). In this connection, there is good evidence that the strong binding of myosin to the thin filament, in the presence of tropomyosin, causes cooperative structural effects on actin itself (43). Identifying these detailed structural changes—as well as the architecture of the native head-to-tail joint—will be an important step in understanding muscle regulation.

We thank L. Tobacman, M. Geeves, P. Vibert, and D. Parry for critical reading of the manuscript, Y. An, Y. Liu, and Y. Song for assistance with the construction of the mutant and with protein expression and purification, M. Love and the staffs of The Cornell High Energy Synchrotron Source and the Brookhaven National Laboratory for assistance with data collection, D. Vassylyev for advice on refinement, and L. Lynch for devotion to the manuscript. This work was supported by grants from the Muscular Dystrophy Association (to C.C.) and from the National Institutes of Health (AR17346 to C.C., GM36326 to S.E.H.D. and N.J.G., HL35726 to S.E.H.D., and 1R01-AR46524–01 to R.D.).

1. Crick, F. H. C. (1953) *Acta Crystallogr.* **6,** 689–697.
2. Cohen, C. & Parry, D. A. D. (1990) *Proteins Struct. Funct. Genet.* **7,** 1–15.
3. Stone, D., Sodek, J., Johnson, P. & Smillie, L. B. (1975) in *Proceedings of the 9th FEBS Meeting* (Akademiai Kiado, Budapest, and North Holland, Amsterdam).
4. Parry, D. A. (1975) *J. Mol. Biol.* **98,** 519–535.
5. McLachlan, A. D. & Stewart, M. (1976) *J. Mol. Biol.* **103,** 271–298.
6. Conway, J. F. & Parry, D. A. D. (1990) *Int. J. Biol. Macromol.* **12,** 328–334.
7. O'Shea, E. K., Klemm, J. D., Kim, P. S. & Alber, T. (1991) *Science* **254,** 539–544.
8. Harbury, P. B., Zhang, T., Kim, P. S. & Alber, T. (1993) *Science* **262,** 1401–1407.
9. Woolfson, D. N. & Alber, T. (1995) *Protein Sci.* **4,** 1596–1607.
10. Lupas, A. (1996) *Trends Biochem. Sci.* **21,** 375–382.
11. Huxley, H. (1972) *Cold Spring Harbor Symp. Quant. Biol.* **37,** 361–376.
12. Parry, D. A. D. & Squire, J. M. (1973) *J. Mol. Biol.* **75,** 33–55.
13. Phillips, G. N., Fillers, J. P. & Cohen, C. (1986) *J. Mol. Biol.* **192,** 111–131.
14. Vibert, P., Craig, R. & Lehman, W. (1997) *J. Mol. Biol.* **266,** 8–14.
15. McKillop, D. F. A. & Geeves, M. A. (1993) *Biophys. J.* **65,** 693–701.
16. Phillips, G. N., Lattman, E. E., Cummins, P., Lee, K. Y. & Cohen, C. (1979) *Nature (London)* **278,** 413–417.
17. Whitby, F. G., Kent, H., Stewart, F., Stewart, M., Xie, X., Hatch, V., Cohen, C. & Phillips, G. N., Jr. (1992) *J. Mol. Biol.* **227,** 441–452.
18. Whitby, F. G. & Phillips, G. N., Jr. (2000) *Proteins Struct. Funct. Genet.* **38,** 49–59.
19. Kunkel, T. A. (1985) *Proc. Natl. Acad. Sci. USA* **82,** 488–492.
20. Hitchcock-DeGregori, S. E. & Varnell, T. A. (1990) *J. Mol. Biol.* **214,** 885–896.
21. Sanger, F., Nicklen, S. & Coulson, A. R. (1977) *Proc. Natl. Acad. Sci. USA* **74,** 5463–5467.
22. Studier, F. W., Rosenberg, A. H., Dunn, J. J. & Dubendorff, J. W. (1990) *Methods Enzymol.* **185,** 60–89.
23. Greenfield, N. J., Montelione, G. T., Farid, R. S. & Hitchcock-DeGregori, S. E. (1998) *Biochemistry* **37,** 7834–7843.
24. Monteiro, P. B., Lataro, R. C., Ferro, J. A. & Reinach, F. D. C. (1994) *J. Biol. Chem.* **269,** 10461–10466.
25. Greenfield, N. J., Stafford, W. F. & Hitchcock-DeGregori, S. E. (1994) *Protein Sci.* **3,** 402–410.
26. Hitchcock-DeGregori, S. E. & Heald, R. W. (1987) *J. Biol. Chem.* **262,** 9730–9735.
27. Urbancikova, M. & Hitchcock-DeGregori, S. E. (1994) *J. Biol. Chem.* **269,** 24310–24315.
28. McLachlan, A. D. & Stewart, M. (1975) *J. Mol. Biol.* **98,** 293–304.
29. Parry, D. A., Crowther, W. G., Fraser, R. D. & MacRae, T. P. (1977) *J. Mol. Biol.* **113,** 449–454.
30. Banner, D. W., Kokkinidis, M. & Tsernoglou, D. (1987) *J. Mol. Biol.* **196,** 657–675.
31. Burkhard, P., Kammerer, R. A., Steinmetz, M. O., Bourkenkov, G. P. & Aebi, U. (2000) *Structure (London)* **8,** 223–230.
32. Walther, D., Eisenhaber, F. & Argos, P. (1996) *J. Mol. Biol.* **255,** 536–553.
33. Gernert, K. M., Surles, M. C., Labean, T. H., Richardson, J. S. & Richardson, D. C. (1995) *Protein Sci.* **4,** 2252–2260.
34. Hammell, R. L. & Hitchcock-DeGregori, S. E. (1996) *J. Biol. Chem.* **271,** 4236–4242.
35. Smillie, L. B. (1999) in *Guidebook to the Extracellular Matrix, Anchor, and Adhesion Proteins*, eds. Kreis, T. & Vale, R. (Oxford Univ. Press, New York), pp. 159–164.
36. Liu, H. & Bretscher, A. P. (1989) *Cell* **557,** 233–242.
37. Anfinsen, C. B. (1973) *Science* **181,** 223–230.
38. Phillips, G. N. & Chacko, S. (1996) *Biopolymers* **38,** 89–95.
39. Mak, A. S., Smillie, L. B. & Stewart, G. R. (1980) *J. Biol. Chem.* **255,** 3647–3655.
40. Bremel, R. D., Murray, J. M. & Weber, A. (1972) *Cold Spring Harbor Symp. Quant. Biol.* **37,** 267–275.
41. Lehman, W., Hatch, V., Korman, V., Rosol, M., Thomas, L., Maytum, R., Geeves, M. A., Van Eyk, J. E., Tobacman, L. S. & Craig, R. (2000) *J. Mol. Biol.* **302,** 593–606.
42. Lehrer, S. S., Golitsina, N. L. & Geeves, M. A. (1997) *Biochemistry* **36,** 13449–13454.
43. Tobacman, L. S. & Butters, C. A. (2000) *J. Biol. Chem.* **275,** 27587–27593.
44. Karibe, A., Tobacman, L. S., Strand, J., Butters, C., Back, N., Bachinski, L. L., Arai, A. E., Ortiz, A., Roberts, R., Homsher, E. & Fananapazir, L. (2001) *Circulation* **103,** 65–71.
45. Parry, D. A. D. (1976) *Biochem. Biophys. Res. Commun.* **68,** 323–328.
46. Kraulis, P. J. (1991) *J. Appl. Crystallogr.* **24,** 946–950.
47. Helfman, D. M., Feramisco, J. R., Ricci, W. M. & Hughes, S. H. (1984) *J. Biol. Chem.* **259,** 14136–14143.